Highly sensitive quantitative detection of water and organic solvent mixtures using a carbon nanotube – paper composite sensor combined with statistical analysis and machine learning techniques

Gregory Philip Moore

A thesis

submitted in partial fulfillment of the

requirements for the degree of

Master of Science

University of Washington

2024

Committee:

Anthony Dichiara, chair

Renata Bura

Richard Gustafson

Program Authorized to Offer Degree:

Environmental and Forest Science

University of Washington

Abstract

Highly sensitive quantitative detection of water and organic solvent mixtures using a carbon nanotube – paper composite sensor combined with statistical analysis and machine learning techniques

Gregory Philip Moore

Chair of the Supervisory Committee:

Dr. Anthony Dichiara

School of Environmental and Forest Sciences

Rapid and quantitative recognition of trace amounts of water in organic solvents is of great importance in industrial operations. Currently the standard methods of determining water content in such cases include the Karl Fischer (KF) titration and fluorescence colorimetry, which are expensive, time consuming, and require skilled operators. In this work, a multifunctional liquid sensing and classification system was developed based on paper comprising pulp fibers adsorbed with multi-walled carbon nanotubes. Papertronics is a field of increasing interest due to the biodegradable nature, flexibility, and light weight of lignocellulosic paper and its ability to be produced at large scale using well-established and cost-effective manufacturing processes. The hygroscopic nature of cellulose fibers causes them to swell radially in response to water molecules, which alters the conductive pathway within the percolated carbon nanotube network present on their surface, leading to a significant change in the paper resistance when wet. Importantly, the

swelling behavior strongly depends on the nature of the solvent, which makes it an exceptional material for liquid sensing applications. The electrical response of the sensor was tested in a classification problem to classify solvents, and a regression problem to quantify concentrations of water in solvents. Specific features were identified from the response profiles, generating over 600 data points which were implemented in the LDA and used to differentiate between the liquids. The sensing platform can classify five different solvents with 100% accuracy and quantify the amount of water in the organic solvent with a limit of detection of 250 ppm and comparable resolution which makes it competitive with the KF titration. The proposed paper-based electronic tongue demonstrates the ability to rapidly differentiate low concentrations of water in organic solvents, provides an economic alternative to current methods, and enables future discoveries in biosensing and bioelectronics.

TABLE OF CONTENTS

LIST OF FIGURES

LIST OF TABLES

LIST OF EQUATIONS

1. Introduction

1.1 Quantitative Recognition of Water in Organic Solvents

Quantitative recognition of trace amounts of water in organic solvents like methanol and ethanol is of great importance in industrial operations such as a biorefinery. In these scenarios, water represents an impurity which lowers the quality and yield of the product, disrupts chemical reaction rates and can cause equipment damage [1]. Currently, the standard method of determining water content in organic solvents is the Karl Fischer titration [2]. This titration involves the use of a Karl Fischer titrator and a KF reagent which contains toxic compounds such as sulfur dioxide, pyridine, and glycol ethers [3]. In addition to these constraints, this approach is also expensive, time consuming and requires skilled operators [4]. Thus, the development of an inexpensive, rapid, and highly sensitive method to determine the water content of organic solvents is necessary.

1.2 Differential Sensing and Electronic Tongue Sensors

Principal Component Analysis (PCA) and Linear Discriminant Analysis (LDA) are related but distinct multivariate statistical techniques which process data that is organized by several correlated variables and reduces the dimensions into two or three new variables, which are not correlated to each other and still retain most of the variation present in the original dataset [5], [6]. Discriminant analysis is commonly used by chemists and bioinformaticians for sensing applications. It is distinct from PCA in that it puts a bias on separating sets belonging to one class from the other classes to maximize separation between the classes and minimize separation within a class [7].

An electronic tongue is a class of electrochemical sensors, which as the name implies, is designed to mimic the human experience of taste. It is a different paradigm in sensing where rather than a

singular, highly selective sensor, an array of low-selective sensors is augmented with advanced signal processing and data analysis [8], [9], [10]. With the growth in machine learning and microcomputing, researchers have improved upon these sensors by providing them with robust object detection and pattern recognition and classification algorithms such as Linear Discriminant Analysis, Principal Component Analysis, Decision Trees, Random Forests, Convolutional Neural Network or Artificial Neural Networks [7], [11].

Gabrieli et al researched polymeric electrochemical sensor arrays which were able to simultaneously quantify the concentrations of multiple cations in aqueous solutions via an extreme-trees machine learning regression model of five features from the differential voltage signal collected by a data acquisition system [12]. de Queiroz et al. found the use of an electronic tongue coupled with principal component analysis to be sufficient to determine water content of ethanol/water mixtures using capacitance measurements on gold electrode sensors [13]. The sensor performed better when tested with tap water than with milliQ water which indicates the ions contribute to the sensing. However, the concentrations of water tested were between 1 to 20% which is still orders of magnitude larger than what can be reasonably achieved with a Karl Fischer titration. There remains a need for a sensor with a below 1% limit of detection of water in organic solvents.

1.3 Decision Trees and Ensemble Machine Learning

Decision trees are a powerful hierarchical machine learning algorithm for classification and prediction tasks. They work by asking series of probing questions that effectively split the classes in data [14]. For classification decision trees, this is achieved by minimizing a cost function, such as the gini impurity, which represents the likelihood of a new data point being misclassified in that

node. A gini impurity of 0 is ideal because it means that class is perfectly separated from the others. Decision trees have a risk of overfitting the data because of their complex nature. This is mitigated by a process known as "pruning" which simplifies the model by removing branches and leaves, and a related process known as "hyperparameter tuning" which defines conditions under which the model can grow. The advantage of decision trees over other models is their easy interpretability over other so-called "black box" models. It is intuitive to understand the rationale behind the model's decisions and tune it accordingly. Similarly, a random forest model takes several decision tree "learners" and has each one vote on the prediction and the prediction with the most votes is reported as the model's prediction [15]. Random forests are part of a group of machine learning models known as ensemble methods which are capable of improving predictive performance and learning complex relationships between the data [16].

1.4 Multifunctional Papertronics and Paper-based Sensing

Cellulose is an insulating polymer and the most abundant biopolymer on Earth, owing to its presence in all plant and tree matter. It has been well studied for over a century for its role in the pulp and paper industry. In the past decade, paper-based sensing devices have taken off for many applications due to their low cost, flexibility, and ease of manufacturing [17]. Witkowska Nery et. al demonstrated a paper-based electronic tongue coupled with K-nearest neighbor algorithm and PCA which was sensitive to four ions present in water and capable of discriminating different water samples [18]. Jiang et al developed a chemiresistive sensor from a graphene-cellulose nanocomposite paper layered on a polymer substrate. A variety of tastes, soft drinks, beers and wines were successfully separated with PCA on eleven descriptive parameters calculated from the resistance signals [19]. Most recently, Amarante et al. developed a printed chemiresistor using

carbon nanotube-cellulose ink which could classify organic solvents and detect glycerin in water by applying a similar approach with multivariate analysis on the descriptive parameters [20].

Conductive polymer composite (CPC) paper can be made by combining the cellulose matrix with conductive nanocarbon such as graphene or carbon nanotubes. This composite has applications in water sensing [21], stress/strain sensors [22], and humidity sensing [23], [24]. Sensors incorporating carbon nanotubes have been extensively researched for flexible circuits and Internet of Things (IoT) connected devices [25]. Recent research has demonstrated the multifunctional "smart" properties of paper which has been embedded with multi-walled carbon nanotubes [26], [27]. Being a naturally hygroscopic material, cellulose swells in the presence of water. This swelling alters the conductive pathway through the material, leading to a measurable change in electrical resistance. Previous research in the Advanced and Sustainable Materials lab by Dr. Sheila Goodman reported the cellulose fibers swell more in water than in ethanol. This preferential swelling to water makes paper-based sensors uniquely suited for selective water detection. From that research it was concluded that the composite paper has "the necessary sensitivity and specificity to detect the presence of water in organic solvents" [28].

The objective of this study is to understand in greater detail the ability of electrically conductive carbon nanotube-paper composite to act as liquid sensors. Two sensor designs will be compared to determine the effect in which the design and sensing mechanism plays a role in the liquid sensing capabilities of the smart paper. The sensors will be tested on a range of classification and water quantification tasks and rigorously analyzed. A robust and repeatable data collection and processing method is presented, and several machine learning and statistical analysis approaches are compared to interpret the signal data from the sensor into meaningful and accurate predictions.

2. Methods and Materials

2.1 Solvent Preparation

Ethanol-based solutions were prepared with Absolute 200 Proof Ethanol from Sigma-Aldrich (Switzerland) while the methanol solutions were prepared using 99.9% methanol from VWR. Reagent grade Acetone >99.5% came from Sigma Aldrich. Isopropanol came from Fischer Chemical. Solvent mixtures for the U-shape tests were prepared at the time of use, so that they would not partially evaporate, which could cause a change in their composition. Solvent mixtures for the strip tests were prepared in falcon tubes which were sealed to mitigate evaporation. Solutions that required mixing were mixed with a magnetic stir rod with a parafilm cover atop the beaker until uniform. If the solution was prepared in a falcon tube, it was mixed on a vortex mixer on the highest setting thoroughly for 20 seconds. For the tests with the U-shape sensor, a syringe was used to fill beakers with the same amount of test solution so that each beakers' liquid was the same height.

2.2 Sensor Preparation and Characterization

The multifunctional paper used in these sensors was prepared in the Wollenberg Paper and Bioresource Science Laboratory following the methods outlined in Dichiara et al [26]. The smart paper sensors were cut to shape using a 1mW laser cutter (Snapmaker, Shenzhen, China) to ensure uniformity. Laser conditions were 65% power, 100% speed, and 1 pass over the material.

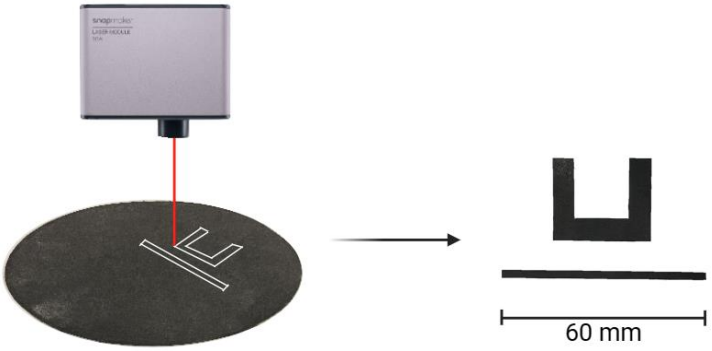

Figure 1. Demonstration of the sensor designs laser cut from a larger sheet of paper. The top sensor is the U-shape, and the bottom is the strip sensor.

At the ends of the strip sensors, 10mm of the paper was adhered to copper tape using silver conductive adhesive (Electron Microscopy Sciences, Hartfield, PA). This improved the contact between the sensors and the copper tape. Alligator clips were clipped to the ends of the copper tape.

Scanning electron microscopy images of the sensor were taken under high vacuum on an Apreo-S electron microscope with a beam voltage of 2.00 kV and a current of 13 pA. Samples of sensor were cut from the paper and adhered to a stage mount using carbon tape.

2.3 Data Acquisition and Testing Hardware and Procedure

For the electrical resistance measurements, alligator clips were connected on both ends of the sensor and the resistance was measured using two wire ohmmeter mode on a Keithley DMM6500 6.5-digit digital multimeter (Tektronix, Beaverton, OR) with a scan rate of 5 readings per second. The digital multimeter was equipped with the Keithley Model 2000-SCAN card to allow for up to

10 channel simultaneous measurements. At the end of testing, the digital multimeter's reading buffer was offloaded to a USB drive for transfer to the computer.

To test the U-shape sensors, a benchtop lab-jack (Precision Scientific, Chicago, IL) raised a beaker of solution towards the sensor until the bottom 7 mm of the sensor was submerged in the liquid. The sensor remained submerged in the liquid for five minutes, after which it was quickly removed from the liquid by lowering the lab-jack. Data collection continued as the sensor dried, until it recovered its initial/dry resistance. Tests were conducted in the fume hood. To ensure uniformity in the testing procedure across samples, special pieces were designed in Fusion360 (Autodesk, San Francisco, CA) and 3D printed using the Snapmaker for the purpose of holding the sensors in place for the duration of the testing. The wetted area of the sensor significantly affects the resistance, so it was crucial that all the sensors were submerged to the same depth so that there was no unwanted variation coming from inconsistencies within the testing procedure.

To test the strip sensors, the sensors were secured in place on glass microscope slides which were subsequently taped down to a hot plate (Corning PC-420D, Glendale, AZ) set to 50°C. The temperature of the hot plate sped up the drying of the sensor which resulted in quicker tests and results. Using a pipette, the volume of the test solution was carefully dropped in the center of each sensor and allowed to wick outward. For the solvent classification experiments, this volume was 7µL. For detecting water in methanol, isopropanol, and ethanol, the test volume was 20µL. Testing continued for a few minutes after the sensor was dry and resistance returned to baseline. Testing was intentionally not done in a controlled humidity environment, to demonstrate the robustness of the sensor to real-world conditions where it would be used. The active area, which is the area of the sensor that gets wet during a test, is roughly the same for both sensor designs.

a) b)

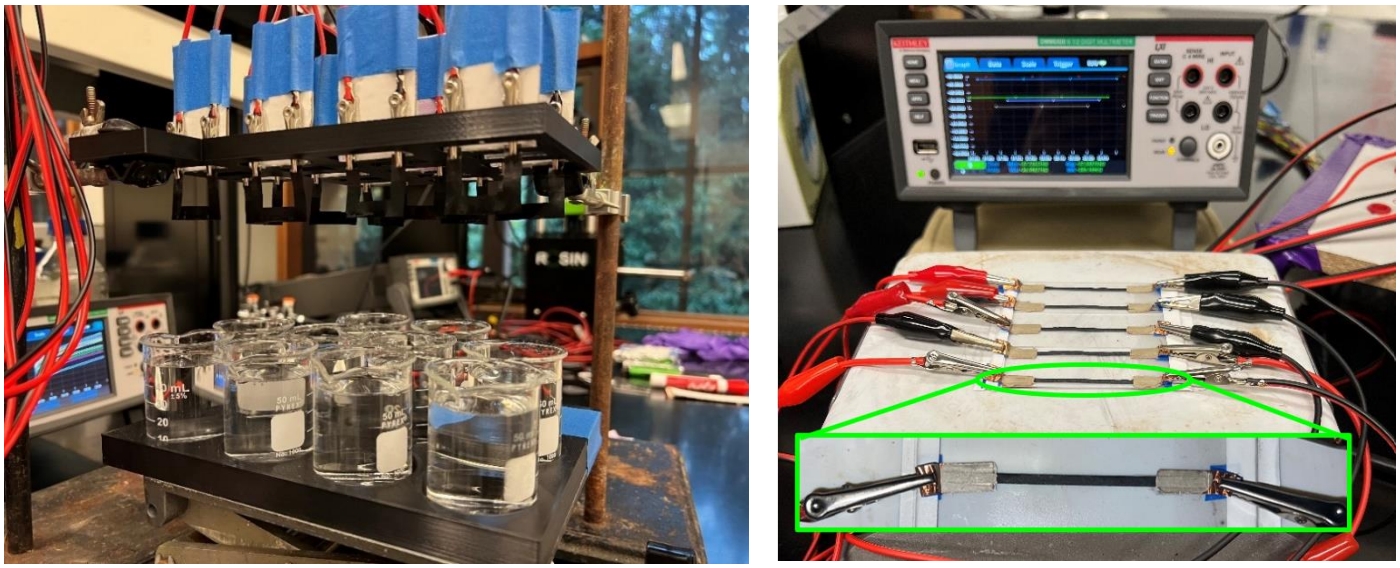

Figure 2. Testing hardware for a) 10-channel simultaneous measurements with the U-shape sensor and b) dropwise experiments with the strip sensor

2.4 Hot Plate Characterization

To ensure uniform heating across the surface of the hot plate, so that different sensors were not unevenly drying, an experiment was conducted to plot the heat map of the two hot plates in the lab. The hot plates were divided into grids of equally spaced squares, a dual laser infrared thermometer (Digisense 20250-08, Cole Palmer, Vernon Hills, IL) was pointed from waist height at the center of each of the squares and the resulting temperature was recorded. This procedure was conducted at 50°C as that was determined to be the temperature used for testing. The characterization of the larger PC620-D hot plate at 40°C and 60°C can be found as Figure 21 in **Appendix C: Hot Plate Characterization.**

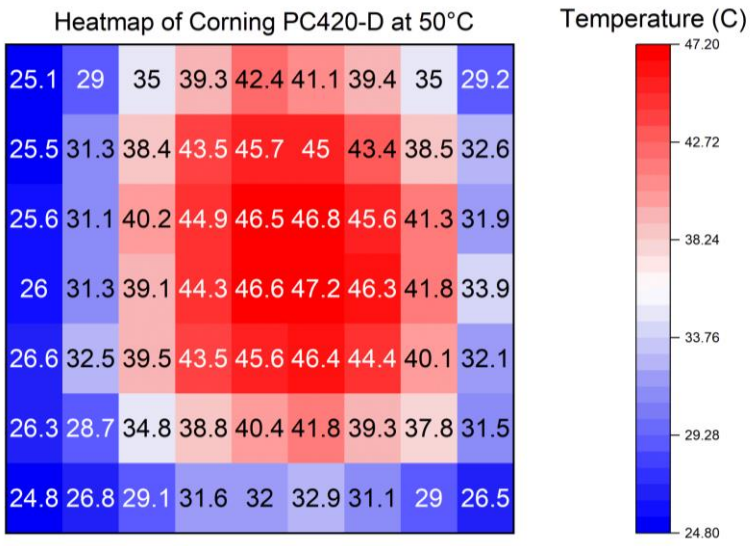

Figure 3. Heatmap of Corning PC420-D Hot Plate set to 50°C

2.5 Experimental Design

The first part of the experiment was to measure the sensors' responses to various solvents to determine the feasibility of classification according to solvent nature. Five solvents were under test for these experiments – Acetone, Ethanol, Isopropanol, Methanol, and Water. To speed up data collection, five different tests ran simultaneously across five different sensors. Each of the sensors saw all the solvents three times for a total of 15 replicates for each solvent.

Table 1. Solvents tested for solvent classification experiments and their properties

Solvent	**Density** $\left(\frac{g}{mL}\right)$	**Surface Tension (mN/m)**	**Heat of Evaporation (kJ/mol)**	**Dielectric Constant**	**Dipole Moment**
Acetone	0.784	25.2	29.1	20.7	2.69
Ethanol	0.789	22.1	42.3	24.55	1.66
Isopropanol	0.785	23.0	45.0	17.9	1.66
Methanol	0.791	22.7	37.6	32.7	2.87
Water	1	72.8	44.0	80.1	1.87

The other experiment was to determine the ability of the sensor to differentiate between concentrations of water in methanol and ethanol. For this, a single sensor was chosen which would be used for all the tests. All test solutions were made up according to the outline in Table 2. Once the sensor was dry, a new sample of test solution would be put into testing and the process would repeat. Methanol was chosen as the first solvent in which to measure the concentration of water. This is because it was found from the solvent classification experiments that methanol had the second highest relative resistance signal from the sensor after water, and we sought to determine the performance of the sensor to quantify water in the highest-resistance organic solvent. Isopropanol, representing an organic solvent with one of the lowest resistances, was also chosen because it was thought that water would be more distinguishable in this solvent, leading to clearer results and predictions.

Table 2. Experimental design of water/solvent mixtures

Sensor Morphology	**Solvent**	**Concentration of DI Water**
U-shape	Methanol	0, 250, 500, 1000, 3000 (ppm)
Strip	Methanol	0, 250, 500, 1000, 3000 (ppm)
U-shape	Isopropanol	0, 250, 500, 1000, 3000 (ppm)
Strip	Isopropanol	0, 250, 500, 1000, 3000 (ppm)
Strip	Ethanol	0, 15%, 25%, 35%, 50%

2.6 Data Processing and Model Building

The data that is output from the multimeter at the end of a test must be processed before it can be used for data analysis. The steps of processing are shown in Figure 4.

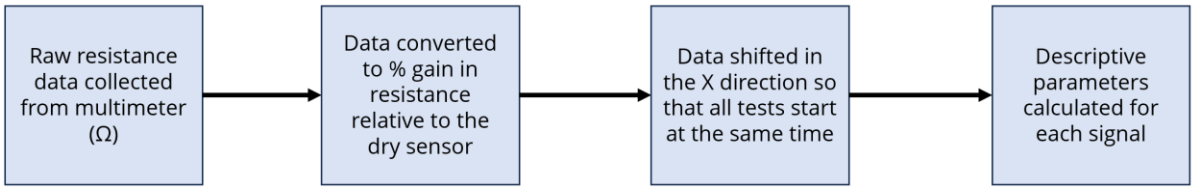

Figure 4. Data processing flowchart

To account for variation in the smart paper sensors, the data is scaled according to the equation below. The change in relative resistance i.e., Gain, (Equation 1) is reported as a percentage increase relative to the baseline resistance of the dry sensor, R_o . R_o is calculated by taking the average of the first five dry resistances. R_t is the wet resistance of the sensor at an instant in time.

$$G\ (\%) = \frac{R_t - R_o}{R_o} * 100$$

Equation 1. Gain (%) in wet resistance relative to dry resistance

From the sensor signal data, several descriptive parameters were determined which were applied in the statistical analysis and machine learning. These parameters were chosen for their ability to uniquely describe the signal. The parameters are labelled on an example signal from the U-shape sensor in Figure 5.

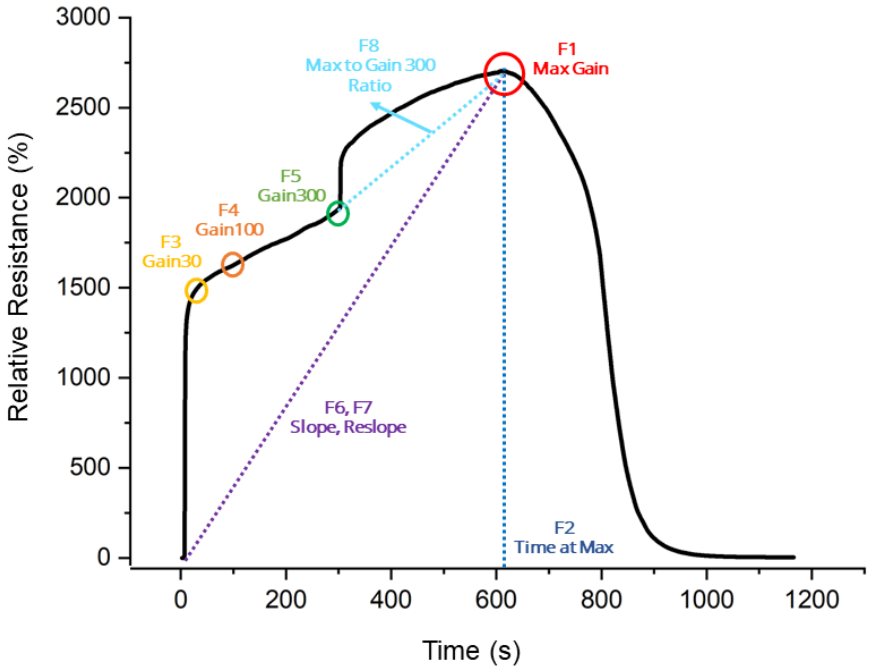

Figure 5. Descriptive parameters F1-F8 extracted from the relative resistance signal

Table 3. Descriptive parameters calculated from sensor signals.

Symbol	Descriptive Parameter	Calculation
F1	Maximum Gain	Max(G)
F2	Time at Max Gain	Tmax(G)
F3	Gain30	Gain at 30 seconds (%)
F4	Gain100	Gain at 100 seconds (%)
F5	Gain300	Gain at 300 seconds (%)
F6	Slope	Max/Tmax
F7	Re-slope	1 / Slope
F8	Max Gain to Gain300 Ratio	Max Gain / Gain300

Much of the machine learning done in this study, including the classification and regression models trained for these experiments, and the scalers used to normalize the data are from the Scikit-learn python package [29]. This package was chosen for its powerful and robust capabilities that span

the entire anatomy of a machine learning project, as well as access to documentation and helpful resources. The trained model and scaler objects are exported and saved via a process known as serialization. This allows the objects to be stored as files on a computer and imported by other pieces of code for later use.

2.7 Multimeter Scripting and Real-time Measurements

The Virtual Instrument Software Architecture (VISA) is an application programming interface (API) which facilitates communication between laboratory equipment and computers. PyVISA is a Python library which allows for VISA commands to be executed in Python [30]. Standard Commands for Programmable Instruments (SCPI) scripting was used with PyVISA to control the digital multimeter from the computer via USB and collect resistance measurements to the computer in real time. At the end of the testing time, the descriptive parameters were calculated immediately, scaled appropriately with the scaler object that had been trained on the data, and compared with the corresponding model for a prediction which was printed to the terminal.

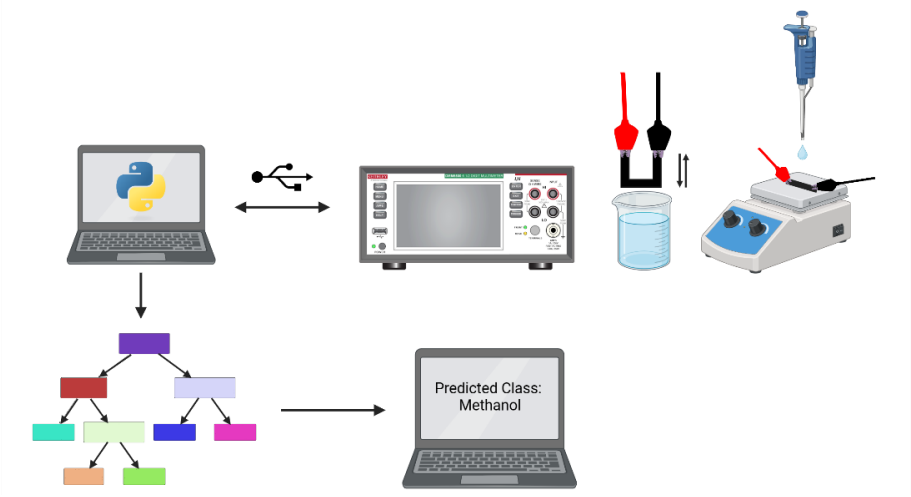

Figure 6. Automated solvent prediction pipeline

3. Results and Discussion

3.1 Sensor Paper Characterization

The paper had an average grammage of 80 grams per square meter and 15 wt% CNT loading. Typical range of sensor resistance was between 20 and 40 kΩ. Figure 7 shows the hierarchical structure of the smart paper, in the lower magnification image one can see the pulp fibers which form the paper, overlapping in multiple directions. The higher magnification image zooms into the interstitial space between the pulp fibers and shows the web-like network of carbon nanotubes which fill in the matrix and cover the cellulose fibers.

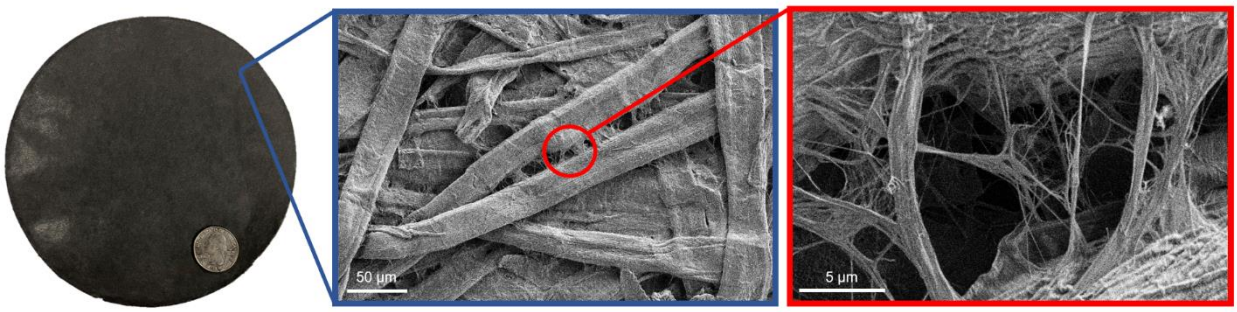

Figure 7. Hierarchical structure of the smart paper under the scanning electron microscope

3.2 Solvent Classification with U-Shape and Strip Sensor

A total of one hundred and fifty tests were conducted, seventy-five for each sensor design, U-shape and strip. From those tests, eight descriptive parameters were calculated, for a total of 600 data points with which to train each classification model. The eight descriptive parameters can be found in *Table 3*. Linear Discriminant Analysis (LDA) was used on the descriptive parameters calculated from the solvent classification experiments with the U-shape and strip sensors. The LDA cluster plot in Figure 8b demonstrates the ability of the U-shape sensor to discriminate water, methanol,

and isopropanol apart from one another, although some overlap occurs between the acetone and the ethanol. With the strip sensor, the classes showed improved separation, as in Figure 8d.

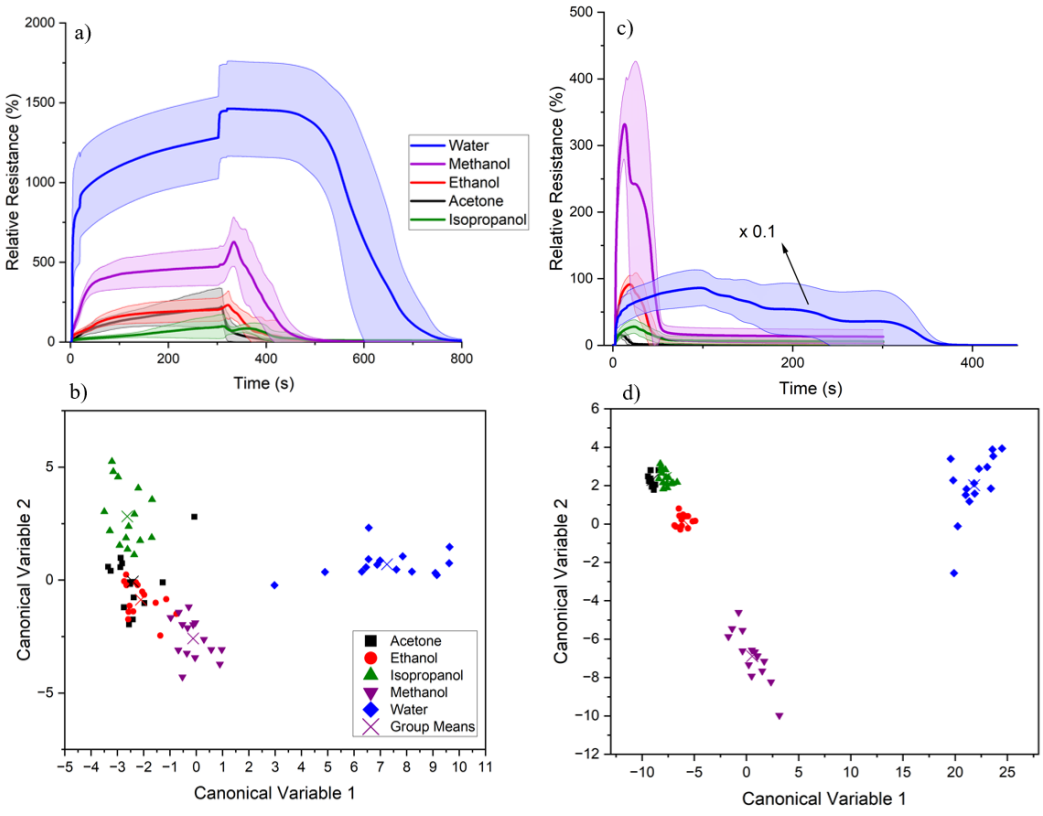

Figure 8. Average ± one standard deviation signals for solvent classification for the U-shape (a) and strip sensor (c), and Linear Discriminant Analysis (LDA) cluster plots for solvent classification with U-shape (b) and strip sensor (d).

3.2.1 Fundamental Understanding of Descriptive Parameters

Certain parameters like gain30 and gain300 have physical meaning behind them. Gain30 represents the gain at 30 seconds which approximately corresponds to the first inflection point in the curve. This could be the transition between the rapid, primary swelling of the cellulose into the more gradual secondary phase of swelling. Gain300 is the gain at 300 seconds which, for the U-

shape sensors' testing method, corresponds to the resistance value at five minutes i.e. right before the sensor is removed from the liquid. The goal with this descriptive parameter is to compare the maximum gain the sensor responds to with each liquid before being removed. The max to gain 300 is a ratio of the maximum gain to the gain at 300 seconds. This descriptive parameter provides useful information on the extent to which the gain continues to increase after the U-shape sensor is removed from the liquid.

Furthermore, the descriptive parameters can encode information about the solvent nature and their physical properties. Figure 9a shows the distribution of the gain300 parameter for the solvents tested for classification with the U-shape sensor and clearly the distributions can be seen to be unique to the solvent, indicating the property of the solvent has something to do with it. From Figure 9b it appears that the gain300 parameter is correlated with the solvent's dielectric constant, with a very high coefficient of determination. The dielectric constant of solvents often indicates the solvent's polarity. A more polar solvent will interact more strongly with the polar hydroxyl and carboxyl groups on the surface of the cellulose fibers. Thus, the higher dielectric constant liquids will disrupt the hydrogen bonds in the cellulose matrix, leading to enhanced swelling and therefore an increase in electrical resistance across the conductive paper.

Likewise, the time-at-max parameter on the strip sensor, in Figure 9c and 9d, is correlated with the surface tension of the solvent. This intuitively can be explained because water has a much higher surface tension than the organic solvents and as such it takes longer to wick into the paper which drags out the time at which the maximum gain occurs. By the time the other solvents have already wicked into the paper and started to evaporate, the water is still in the process of wicking or on the surface of the paper.

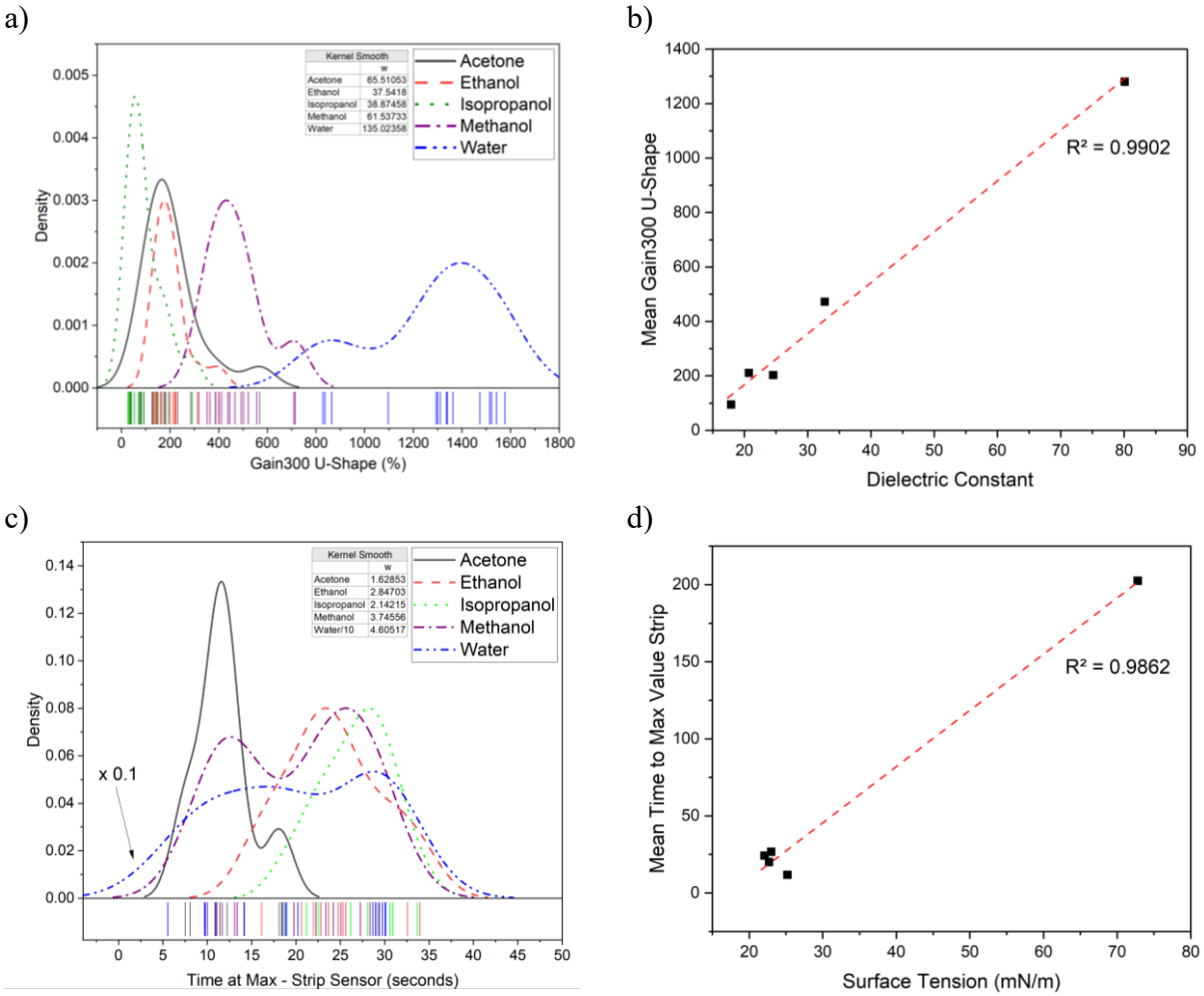

Figure 9. a) Distribution of gain300 parameter for different solvents on U-shape sensor, b) Scatter plot of relationship between dielectric constant and gain300, c) Distribution of time-at-max parameter on strip sensor, d) Scatter plot of relationship between surface tension and time-at-max.

3.2.2 Solvent Classification Decision Trees

A Decision Tree Classifier from `sklearn.tree` was selected as the model for these experiments. A separate classification model was trained for each sensor design. Python 3.10 was used to process the data and train the models. The data was scaled with `StandardScaler` from `sklearn.preprocessing` so that each feature has a mean of zero and a standard deviation of one. This is done so that models aren't placing extra importance on features with larger numbers,

and rather they are assigning importance to features because of the effect they have on the variation in the data. After scaling, the data was split into training and testing data with a test split of 20%. `GridSearchCV` with 5-fold cross validation was used to determine each model's optimal hyperparameters, those which gave the highest accuracy and F-1 metrics. However, to avoid unnecessary complexity and overfitting, the model was simplified and generalized by regularizing the parameters. A summary of the models' hyperparameters and evaluation metrics is presented in *Table 4*.

Table 4. Summary of model hyperparameters and metrics for U-shape and strip sensors

	U-Shape Sensor Decision Tree Classifier	**Strip Sensor Decision Tree Classifier**
"Max_depth"	3	3
"Min_samples_split"	3	3
"Min_samples_leaf"	11	10
F-1 Score	93.6%	100.0%
Training Accuracy	95.0%	100.0%
Testing Accuracy	93.3%	100.0%

The decision trees were visualized and reported in Figures 10 and 11. The values in the brackets of each node indicate the number of instances belonging to each class that were present in the training data [Acetone, Ethanol, Isopropanol, Methanol, Water]. As can be seen in Figure 10, the gain100 parameter was used by the root node to split water and methanol from the other solvents. In the second decision node the gain300 parameter was used to split the methanol from the water. Likewise, the gain300 parameter was used to separate the isopropanol from acetone and ethanol. Acetone and ethanol appeared to be the two most similar solvents for the sensor to distinguish, as they needed another question node to separate them, and even still their gini impurity scores were

0.298 and 0.153 respectively. Comparing the average signals for each of the solvents in Figure 9a shows that the ethanol and acetone signals are the most similar. Furthermore, this is also consistent with the findings in Goodman et al [27] which demonstrates those two solvents have similar R_{rel} @ 300s. The similarity of these solvents could contribute to their misclassification.

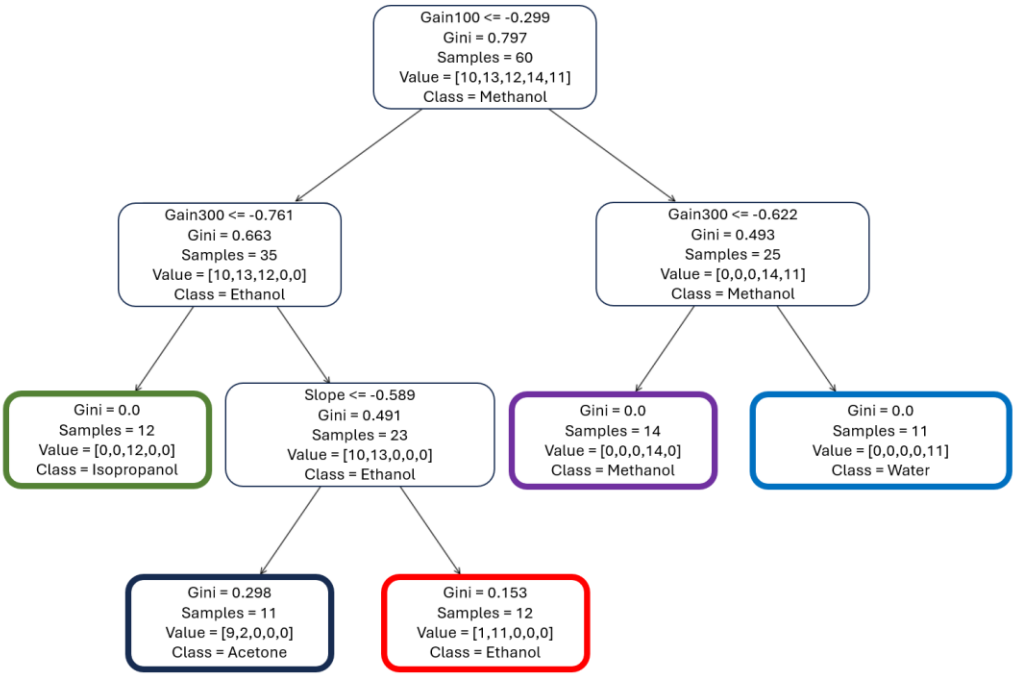

Figure 10. Decision tree classifier used for solvent classification with the U-shape sensor

In Figure 11 it is apparent that, with the strip sensor, a relatively simple model with only a depth of three can perfectly distinguish the five solvents from one another with no misclassifications.

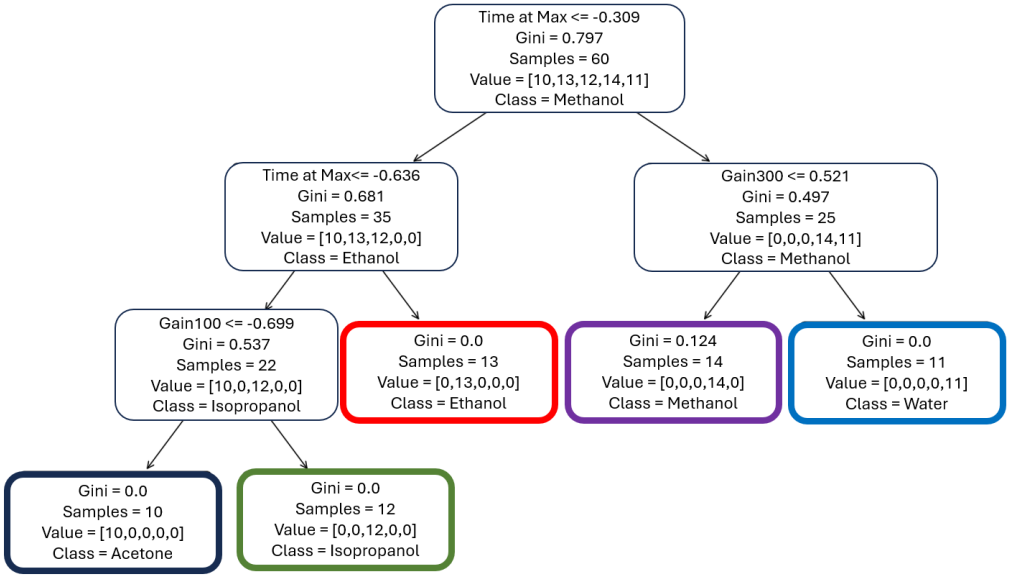

Figure 11. Decision tree classifier used for solvent classification with the strip sensor

3.2.2 Confusion Matrices of Solvent Classification Decision Trees

The confusion matrix is a common tool in classification tasks to visualize classification accuracy and spot areas where a model may be underperforming. For both models, separate confusion matrices were computed for the results on the training dataset and those on the testing dataset. Results were normalized to be expressed as a percentage of the total number of values belonging to each class. A perfect confusion matrix looks like the two in the right-hand column of Figure 12, corresponding to the strip sensor, where there are only values present along diagonals of the matrix and none elsewhere.

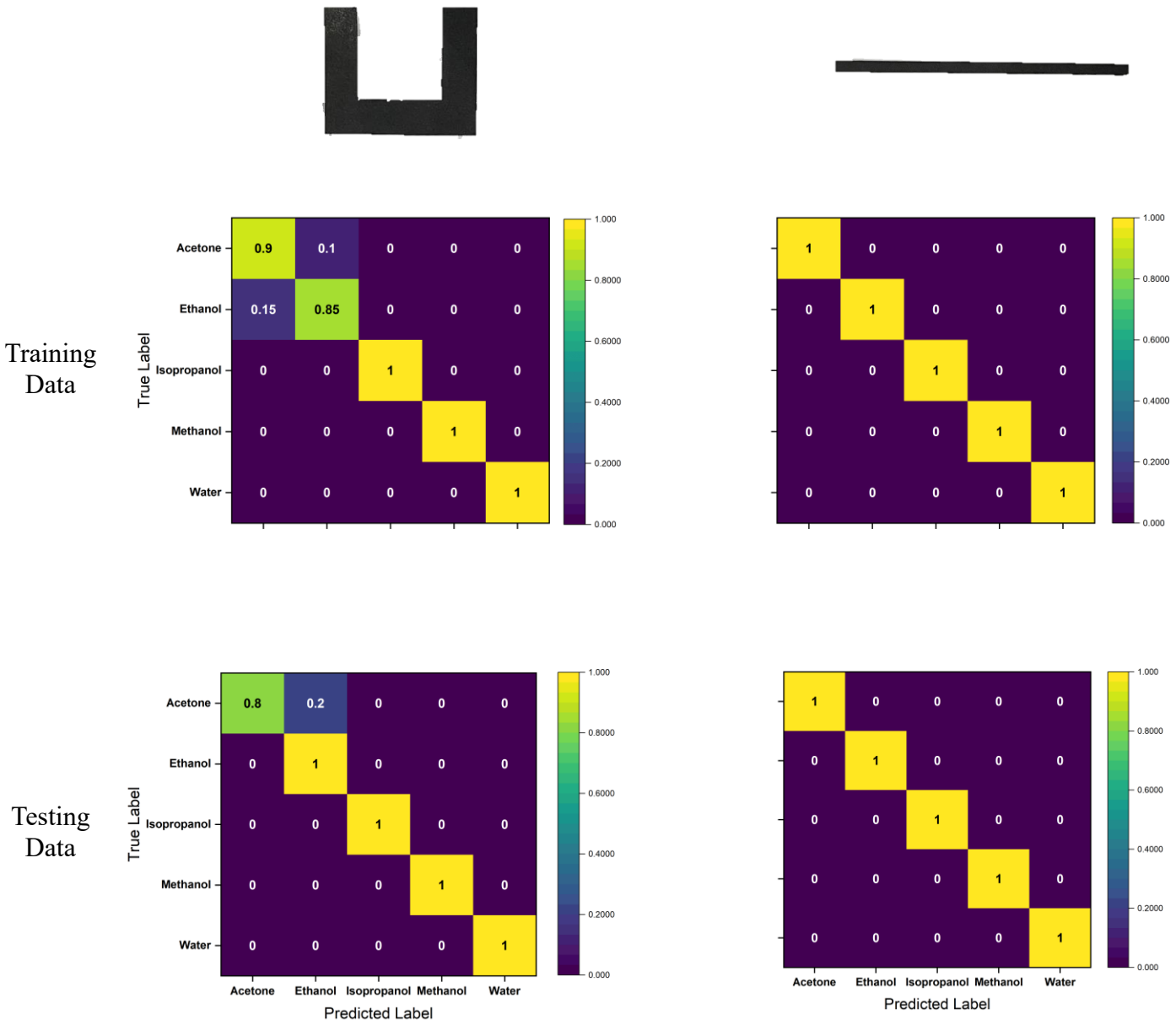

Figure 12. Normalized confusion matrices for the training and testing data from the solvent classification experiments with U-shape and strip sensors.

3.3 Sensor Design Performance

The data from the solvent classification experiments was used to determine the robustness and reliability of the sensors. The data represents the responses of ten different sensors (five U-shape and five strip) each tested three separate times for each solvent. The ratio of the max gain parameter for each solvent relative to the max gain parameter for isopropanol was computed. The results were normalized to have a mean of 0 and a standard deviation of 1 and plotted on distribution plots in Figure 13 . It appears that the U-shape sensor exhibits a narrower distribution indicating that it is possibly more consistent than the strip sensor. Furthermore, on the U-shape sensor there is a predicable narrower distribution between the organic solvents and IPA as compared to water and IPA. This is indicative of the variation of maximum values of water being higher than for organic solvents. Both sensor designs have a tail of higher values between +2 to +3 standard deviations from the mean. Further research will need to be done on the cause of this, as it could have implications for the sensor design.

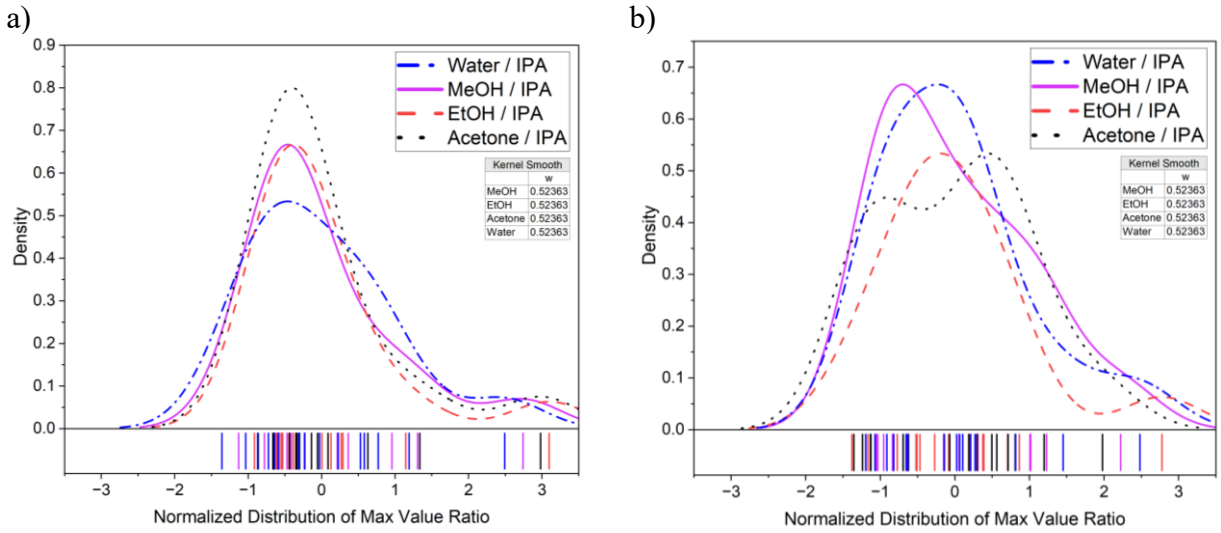

Figure 13. Distributions of ratio of max value parameter, normalized with a mean of 0 and standard deviation of 1 for a) U-shape sensor and b) strip sensor.

The full-width half maximum (FWHM) from the distribution of the ratio of water/isopropanol max value was computed. This value can be interpreted as a quantitative metric of the sensor's reliability. A smaller FWHM indicates the sensor is more consistent in how it responds to water relative to isopropanol. This is an important characteristic for the sensor to work well in the next sections to detect and quantify concentrations of water in organic solvents. For the U-shape sensor the FWHM was 1.50745 for the ratio of water/isopropanol, for the strip sensor it was 0.66811. This means that the U-shape sensor returned more variable results than the strip sensor.

A side-by-side comparison of the two sensors along five important metrics is represented by the spider plot in Figure 14. The evaluation metrics are the time needed to complete a test, volume of liquid needed for the test, the accuracy and F1 scores of the solvent classification models trained from the sensors, and the FWHM.

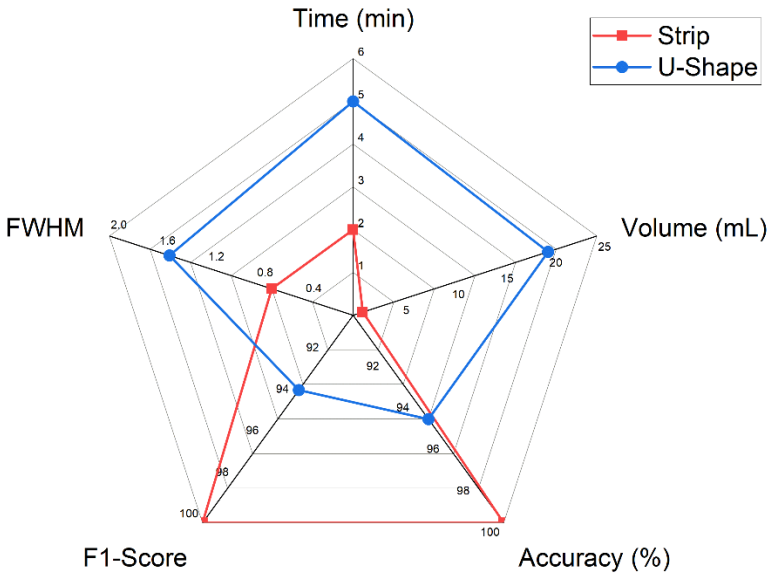

Figure 14. Spider plot comparison of the U-shape and strip sensors

3.4 Detection of Water in Methanol with U-Shape and Strip Sensors

The ability of the sensor to determine the concentration of water in methanol was investigated in this section. The U-shape sensor showed good separation of pure methanol, 250 ppm, 500 ppm, 1000 ppm, and 3000 ppm water in methanol. This indicates the sensor was able to detect water concentrations as low as 250 ppm as being different from pure methanol, indicating a possible limit of detection of 250 ppm. However, as can be seen in Figure 15a, the clusters corresponding to 500 ppm and 1000 ppm partially overlap, possibly indicating a detection resolution of ± 500 ppm. The parameters used for the discriminant analysis with the U-shape sensor were maximum gain, time at max, slope, gain30, and gain100. The parameters used for discriminant analysis with the strip sensor were maximum gain, gain10, gain15, gain20, and gain 25. The strip sensor in Figure 15b exhibited separation between 0 ppm and 250 ppm however the clusters belonging to 250 ppm and 500 ppm and intertwined so there may not be good resolution.

a)

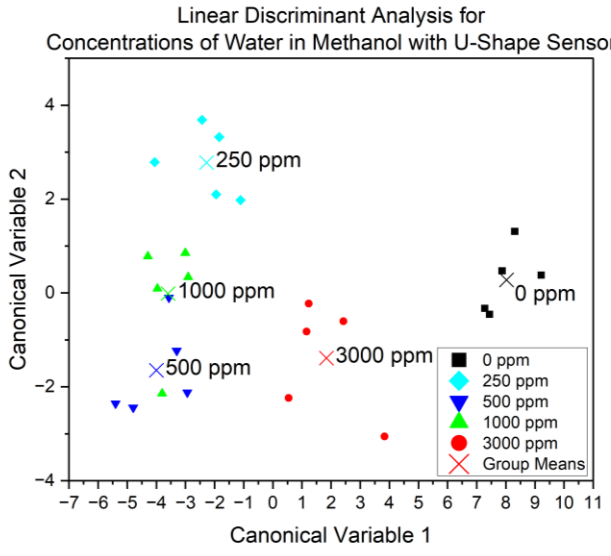

b)

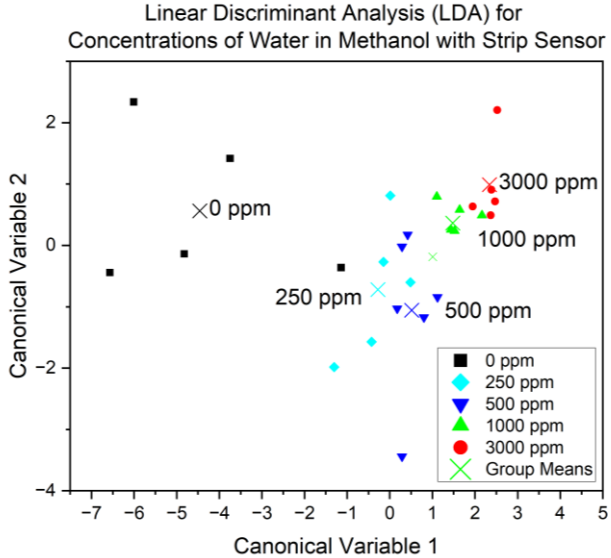

Figure 15. Linear Discriminant Analysis (LDA) plots for various concentrations of water in methanol using a) U-shape sensor and b) strip sensor.

3.5 Detection of Water in Isopropanol with U-Shape and Strip Sensors

The ability of the sensor to determine the concentration of water in isopropanol was investigated in this section. The parameters used for the discriminant analysis with the U-shape sensor were maximum gain, time at max, slope, reslope, and gain30. The parameters used for the discriminant analysis with the strip sensor were maximum gain, slope, gain10, gain20, gain30. Seen in Figure 16a, the U-shape sensor showed good separation of the 0 ppm and 250 ppm as well as the 1000 ppm and 3000 ppm. The strip sensor also showed better separation between all the classes. The relative location of the clusters to one another is different between the U-shape and strip plots, but this is to be expected because the axes represent combinations of different parameters. Comparing these results to those in **3.4 Detection of Water in Methanol with U-Shape and Strip Sensors,** the U-shape sensor performed similarly in that they were both able to tell apart 0 ppm from 250 ppm from 500 ppm. On the strip sensor, the water in isopropanol had better clustering than the water in methanol. This may be a result of isopropanol having a smaller signal than methanol (see Figure 8a), i.e. the isopropanol is more “different” from water than the methanol is. This makes the fractional concentrations of water more easily detectable by the sensor, allowing for a lower limit of detection and finer resolution than with the methanol in water. Further results are reported in the next section with water in ethanol, as ethanol represents a solvent “in-between” isopropanol and methanol

a) b)

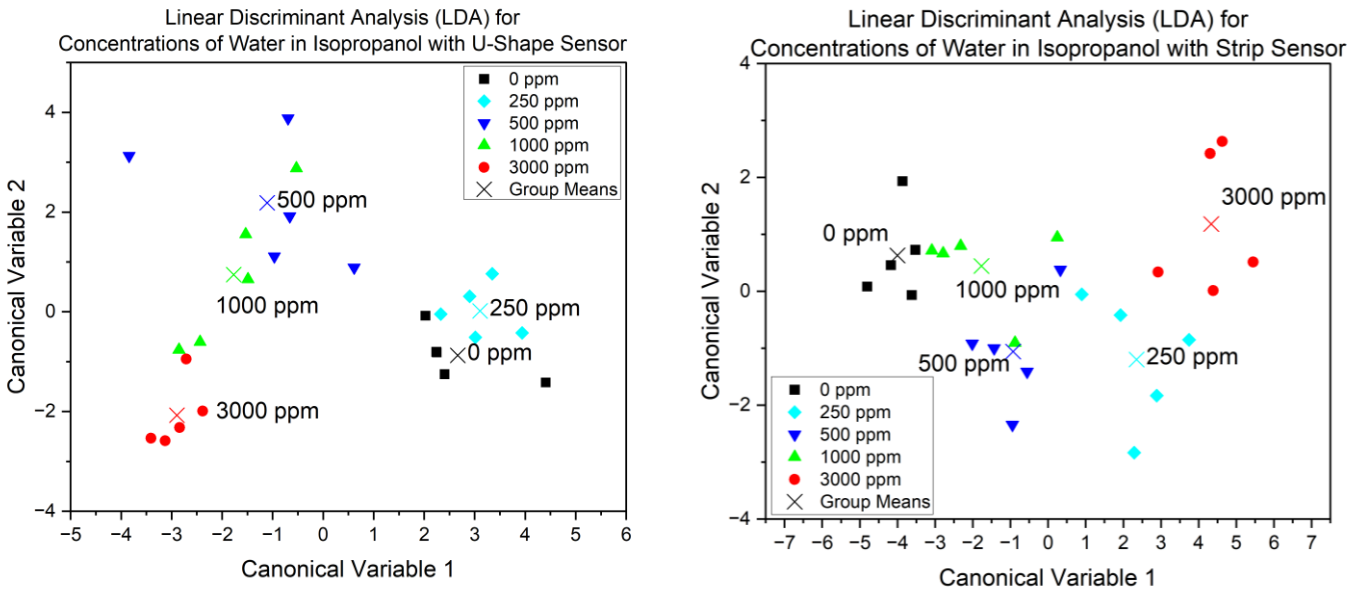

Figure 16. Linear Discriminant Analysis (LDA) plots for various concentrations of water in isopropanol using a) U-shape sensor and b) strip sensor.

3.6 Quantitative Recognition of Water Concentration in Ethanol

The ability of the strip sensor to quantify the concentration of water in ethanol was experimented. Initially the sensor was tested on pure ethanol and pure water, as well as mixtures of 15%, 25%, 35%, 50%, and 75% water in ethanol. In the same setup as the solvent classification experiments, five strip sensors were tested to collect the data. As shown in the next section, the data belonging to 75% water in ethanol were removed from consideration and not used for training a regression model.

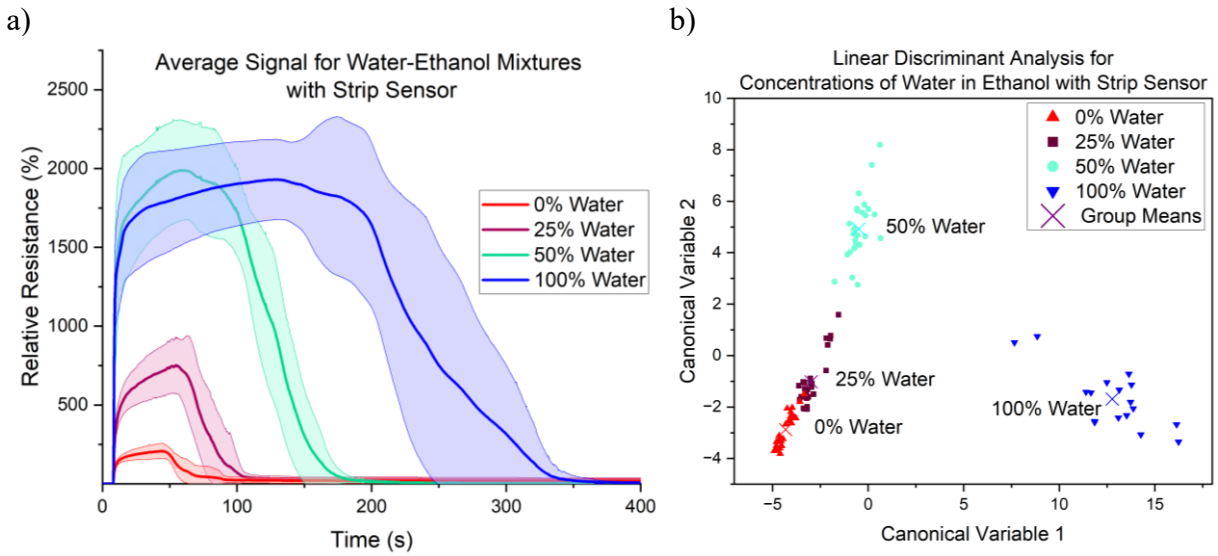

Figure 17. a) Average signals for water-ethanol mixtures with the strip sensor, shaded region represents ± one standard deviation, b) LDA cluster plot

3.6.1 Decision Tree and Random Forest Classification

Decision tree and random forest classification models were trained on the data to establish a baseline of the sensor's ability to tell apart the different concentrations. The following descriptive parameters were used to train the models: max_gain, time_max, slope, reslope, gain30, gain50, gain100, gain200, and gain300. Following the same grid search 5-fold cross-validation approach as used in the solvent classification, the optimal hyperparameters for each model were found and are reported in Table 5.

Table 5. Model hyperparameters and evaluation metrics (including 75% water in ethanol)

	Decision Tree	**Random Forest**
“Max_depth”	4	4
“Min_samples_leaf”	5	1
“Min_samples_split”	5	9
“N_estimators”	-	25
F1 Score	0.853	0.846
Training Accuracy	0.904	0.923
Testing Accuracy	0.846	0.846

The random forest model had a slightly improved training accuracy over the decision tree classifier. However, since both models can be prone to overfitting, the more important metric is the F1 score and the testing accuracy in which the random forest model did not improve upon the decision tree. For this reason, the random forest model was not considered to be a better model.

The low accuracies and F1 scores for both models can be attributed to misclassifications between 50% water in ethanol and 75% water in ethanol. This possibly indicates that the current sensor and testing method is most accurate for mixtures of water and ethanol where water represents the minority constituent (≤ 50%). Future work will need to be done to develop a method to sense liquid mixtures where water is the majority constituent (>50%). The data points belonging to 75% water in ethanol were removed and more data was collected at 0%, 25% and 50%. The model was retrained on the expanded dataset and yields the decision tree in Figure 18, which has no misclassifications between the concentrations and reports a 100% accuracy on the training and testing sets, as well as an F1 score of 1.00.

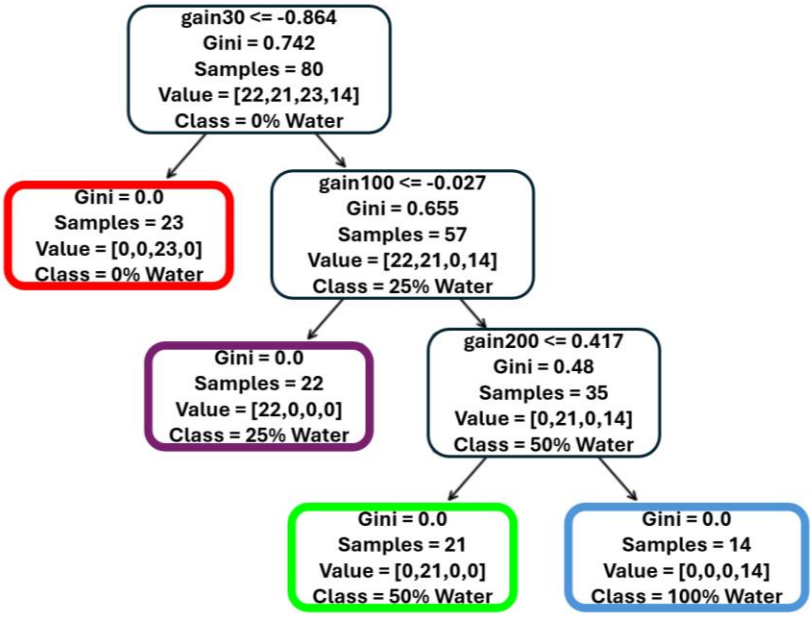

Figure 18. Decision Tree Classifier for water ethanol mixtures where water represents the minority constituent.

3.6.2 Multiple Linear Regression

A multiple linear regression model was trained on the data, with the X variables being the descriptive parameters and the output variable a number between 0 and 1 representing the weight percent water of the water/ethanol mixtures. Additional data points were collected at concentrations of 15% and 35% water in ethanol to make the linear regression more complete. The coefficients of the model are represented as a linear equation in *Equation 2*. The metrics used to evaluate the model's performance are summarized in *Table 6*.

$$wt\ \%\ Water = 0.248 - 0.073x_1 + 0.087x_2 + 0.089x_3 - 0.056x_4 - 0.020x_5 + 0.112x_6 - 0.009x_7 - 0.045x_8 + 0.014x_9$$

Equation 2. Multiple linear regression equation relating the weight % water in the mixture to the descriptive parameters of the resistance signal

Table 6. Performance metrics for multiple linear regression model

R^2 Score	0.936
Mean Squared Error	0.0019
Mean Absolute Error	0.0351

On the 20% of data which was set aside for testing and not seen by the model during training, predicted water concentrations were computed by the trained model. The range of predicted values at each concentration and the average of the predictions is represented by the violin plot in Figure 19. At the extremes of the testing window; 0% and 50%, the distribution is narrower and the predicted values are more precise to one another. The middle concentrations, especially 25%, still have a wide variation in the predicted values. The partial overlap between 15%, 25%, and 35% could indicate that collecting training data across five different sensors introduced enough variability to obfuscate the variation caused by ± 10% water in the solvent. In other words, the variation caused by a 10% change of water was partially lost in the within-group variation due to the multiple sensors. This could have implications for the sensor manufacturing and ensuring uniform performance.

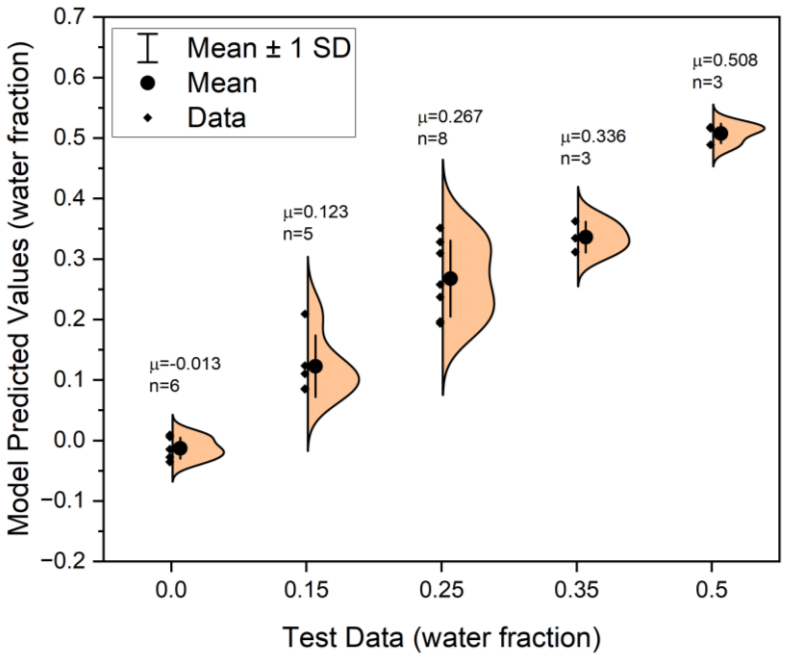

Figure 19. Violin plots of predicted values for the linear regression model on the test data

3.6.3 Live Testing and Model Validation

Following the procedure in **2.7 Multimeter Scripting and Real-time Measurements**, several live validation tests were performed with the sensor connected to the trained multiple linear regression model via PyVISA. The known concentration of the mixture as it was prepared, as well as the corresponding predicted concentrations are reported in *Table 7.* The concentrations were chosen to be the concentrations which the model was trained on, as well as two (7% and 42%) to represent in-between values to validate the model's ability to interpolate and quantify new concentrations which it hasn't seen before.

Table 7. Model performance validation and difference between actual and predicted concentrations

Actual Concentration (%)	Predicted Concentration from MLR Model (%)	% Difference
0	-1.57	-1.57
0	-3.375	-3.375
0	-2.653	-2.653
7	1.00	-6.00
7	1.74	-5.26
7	1.04	-5.96
15	8.857	-6.143
15	13.88	-1.12
15	8.382	-6.618
25	19.115	-5.885
25	22.5817	-2.4183
25	25.414	0.414
35	30.988	-4.012
35	32.055	-2.945
35	32.637	-2.363
42	35.51	-6.49
42	37.07	-4.93
42	35.17	-6.83
50	45.618	-4.382
50	42.472	-7.528
50	37.028	-12.972

This data is represented by the histogram in Figure 20. Across all validation tests the model most frequently predicted between 3-6% less water in ethanol than what the known concentration of water in ethanol. With the exception of an outlier, the distribution is narrow. This indicates that while the sensor may be off by a few percent, it is consistent in its predictions.

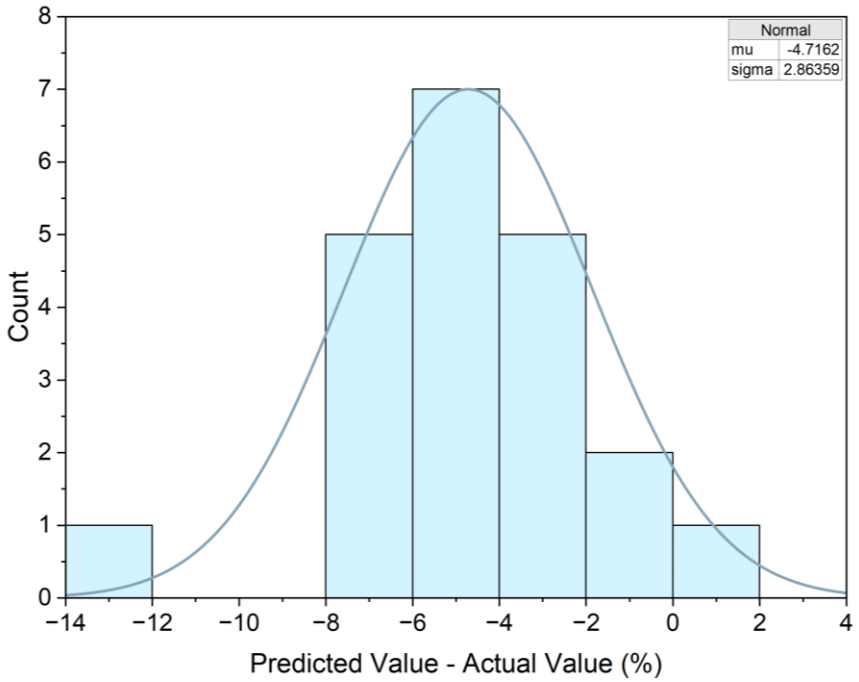

Figure 20. Histogram of sensor-model validation difference between actual and predicted values

4. Conclusion

In this work two designs of the electrically conductive paper sensor were developed and compared for their performance on liquid classification and water quantification tasks. In all metrics evaluated, the strip sensor performed better than the U-shape sensor. This sensor design took less time to get a result, required less volume of solvent, was more accurate in its results, and performed more reliably.

It is proposed that the sensing mechanism in which the smart paper works is different for the two sensor morphologies. The predominant mechanism for the U-shape sensor is the swelling of the cellulose fibers as the paper is exposed to the liquid for a longer period and has more time to swell

in response. The strip sensor by contrast, is possibly driven by liquid properties and wicking. While the active area of the sensors is the same, the strip sensor is wet for a much shorter period so there may not be adequate time for a thorough swelling of the cellulose fibers. Other solvent properties such as the surface tension or the dielectric constant were shown to have a strong effect on the sensor's responses to the liquids and the descriptive parameters calculated therein.

The sensor demonstrated the ability to classify five different solvents from one another with a simple decision tree classification model. The sensor also showed a detection resolution of 250 ppm water in methanol as well as 250 ppm water in isopropanol.

Lastly, several regression models were compared for their ability to predict the concentration of water in ethanol using the strip sensor. Using a robust data processing workflow that was developed, live tests are conducted from the computer connected to the multimeter and predictions were reported in minutes within ± 10%.

5. Future Work

As with any data science application, the strength of the models you can build and the conclusions you can draw is dependent on the quantity and quality of data you can collect. As such, there is always the need to collect more data and develop new data collection procedures. These could help train more powerful models like neural networks or random forests. With these more powerful models perhaps the sensor's limit of detection and resolution could be improved.

Furthermore, the solvent classification experiments were far from exhaustive, and the sensor could be tested with more solvents that weren't included in the original set. One practical example is testing for the presence of water in gasoline, either through a regression/quantification algorithm

or even a simple binary algorithm (water detected / no water detected). There is also an opportunity for more work to be done on the testing conditions and determining better procedures that help improve the specificity of the model. For example, changing the amount of time the U-shape sensor is submerged in the liquid. In this study, the sensor was submerged only for 5 minutes, however perhaps a longer time like 10 or 15 minutes would help the sensor tell apart different concentrations of water reliably. Likewise, for the strip sensor, the hot plate temperature can be changed from 50°C to determine if there is a more suitable temperature.

As for the sensor material and design, different functionalization on the smart paper, or arrays of sensors working in parallel could open new realms in sensing that were not yet achieved in this study.

The quality of the linear regression model and the accuracy of the predictions of water concentration were limited by the fact that the data was collected on five sensors. More work will need to be done collecting the data all on the same sensor which will lead to a smaller resolution of detection.

References

[1] J. Martinka, P. Rantuch, and I. Wachter, “Impact of Water Content on Energy Potential and Combustion Characteristics of Methanol and Ethanol Fuels,” *Energies*, vol. 12, no. 18, Art. no. 18, Jan. 2019, doi: 10.3390/en12183491.

[2] E. Scholz, *Karl Fischer Titration: Determination of Water Chemical Laboratory Practice*. Springer-Verlag, 1984.

[3] “Standard Test Method for Water Using Volumetric Karl Fischer Titration.” Accessed: Aug. 28, 2023. [Online]. Available: https://www.astm.org/e0203-16.html

[4] D. Surangsrirat *et al.*, “Non-destructive measurement technique for water content in organic solvents based on a thermal approach,” *RSC Adv.*, vol. 12, no. 10, pp. 6181–6185, doi: 10.1039/d2ra00352j.

[5] J. E. Jackson, *A User’s Guide to Principal Components*. in Wiley Series in Probability and Mathematical Statistics. Wiley-Interscience, 1991.

[6] I. T. Jolliffe, *Principal Component Analysis*, Second. in Springer Series in Statistics. 2002.

[7] S. Stewart, M. Adams Ivy, and E. V. Anslyn, “The use of principal component analysis and discriminant analysis in differential sensing routines,” *Chem. Soc. Rev.*, vol. 43, no. 1, pp. 70–84, 2014, doi: 10.1039/C3CS60183H.

[8] Y. Vlasov, A. Legin, A. Rudnitskaya, C. D. Natale, and A. D’Amico, “Nonspecific sensor arrays (‘electronic tongue’) for chemical analysis of liquids (IUPAC Technical Report),” *Pure Appl. Chem.*, vol. 77, no. 11, pp. 1965–1983, Jan. 2005, doi: 10.1351/pac200577111965.

[9] M. del Valle, “Electronic Tongues Employing Electrochemical Sensors,” *Electroanalysis*, vol. 22, no. 14, pp. 1539–1555, 2010, doi: 10.1002/elan.201000013.

[10] M. del Valle, “Sensor Arrays and Electronic Tongue Systems,” *Int. J. Electrochem.*, vol. 2012, p. e986025, Feb. 2012, doi: 10.1155/2012/986025.

[11] F. Cui, Y. Yue, Y. Zhang, Z. Zhang, and H. S. Zhou, “Advancing Biosensors with Machine Learning,” *ACS Sens.*, vol. 5, no. 11, pp. 3346–3364, Nov. 2020, doi: 10.1021/acssensors.0c01424.

[12] G. Gabrieli *et al.*, “Combining an Integrated Sensor Array with Machine Learning for the Simultaneous Quantification of Multiple Cations in Aqueous Mixtures,” *Anal. Chem.*, vol. 93, no. 50, pp. 16853–16861, Dec. 2021, doi: 10.1021/acs.analchem.1c03709.

[13] D. P. de Queiroz, A. de O. Florentino, J. C. Bruno, J. H. D. da Silva, A. Riul, and J. A. Giacometti, “The use of an e-tongue for discriminating ethanol/water mixtures and determination of their water content,” *Sens. Actuators B Chem.*, vol. 230, pp. 566–570, Jul. 2016, doi: 10.1016/j.snb.2016.02.080.

[14] Y. SONG and Y. LU, “Decision tree methods: applications for classification and prediction,” *Shanghai Arch. Psychiatry*, vol. 27, no. 2, pp. 130–135, Apr. 2015, doi: 10.11919/j.issn.1002-0829.215044.

[15] L. Breiman, “Random Forests,” *Mach. Learn.*, vol. 45, no. 1, pp. 5–32, Oct. 2001, doi: 10.1023/A:1010933404324.

[16] O. Sagi and L. Rokach, “Ensemble learning: A survey,” *WIREs Data Min. Knowl. Discov.*, vol. 8, no. 4, p. e1249, 2018, doi: 10.1002/widm.1249.

[17] E. W. Nery and L. T. Kubota, “Sensing approaches on paper-based devices: a review,” *Anal. Bioanal. Chem.*, vol. 405, no. 24, pp. 7573–7595, Sep. 2013, doi: 10.1007/s00216-013-6911-4.
[18] E. Witkowska Nery, J. A. Guimarães, and L. T. Kubota, “Paper-Based Electronic Tongue,” *Electroanalysis*, vol. 27, no. 10, pp. 2357–2362, 2015, doi: 10.1002/elan.201500054.
[19] X. Jiang *et al.*, “Rapid Liquid Recognition and Quality Inspection with Graphene Test Papers,” *Glob. Chall.*, vol. 1, no. 6, p. 1700037, 2017, doi: 10.1002/gch2.201700037.
[20] T. Amarante *et al.*, “Carbon nanotube-cellulose ink for rapid solvent identification,” *Beilstein J. Nanotechnol.*, vol. 14, pp. 535–543, Apr. 2023, doi: 10.3762/bjnano.14.44.
[21] H. Qi, E. Mäder, and J. Liu, “Unique water sensors based on carbon nanotube–cellulose composites,” *Sens. Actuators B Chem.*, vol. 185, pp. 225–230, Aug. 2013, doi: 10.1016/j.snb.2013.04.116.
[22] M. Khalifa, G. Wuzella, H. Lammer, and A. R. Mahendran, “Smart paper from graphene coated cellulose for high-performance humidity and piezoresistive force sensor,” *Synth. Met.*, vol. 266, p. 116420, Aug. 2020, doi: 10.1016/j.synthmet.2020.116420.
[23] P. Zhu *et al.*, “Flexible and Highly Sensitive Humidity Sensor Based on Cellulose Nanofibers and Carbon Nanotube Composite Film,” *Langmuir*, vol. 35, no. 14, pp. 4834–4842, Apr. 2019, doi: 10.1021/acs.langmuir.8b04259.
[24] R. Barras, I. Cunha, D. Gaspar, E. Fortunato, R. Martins, and L. Pereira, “Printable cellulose-based electroconductive composites for sensing elements in paper electronics,” *Flex. Print. Electron.*, vol. 2, no. 1, p. 014006, Mar. 2017, doi: 10.1088/2058-8585/aa5ef9.
[25] J. A. Cardenas, J. B. Andrews, S. G. Noyce, and A. D. Franklin, “Carbon nanotube electronics for IoT sensors,” *Nano Futur.*, vol. 4, no. 1, p. 012001, Jan. 2020, doi: 10.1088/2399-1984/ab5f20.
[26] A. B. Dichiara, A. Song, S. M. Goodman, D. He, and J. Bai, “Smart papers comprising carbon nanotubes and cellulose microfibers for multifunctional sensing applications,” *J. Mater. Chem. A*, vol. 5, no. 38, pp. 20161–20169, 2017, doi: 10.1039/C7TA04329E.
[27] S. M. Goodman *et al.*, “Scalable manufacturing of fibrous nanocomposites for multifunctional liquid sensing,” *Nano Today*, vol. 40, p. 101270, Oct. 2021, doi: 10.1016/j.nantod.2021.101270.
[28] S. M. Goodman, “Sustainable Cellulose Composite Membranes for Multifunctional Sensing Applications”.
[29] F. Pedregosa *et al.*, “Scikit-learn: Machine Learning in Python,” *J. Mach. Learn. Res.*, vol. 12, no. 85, pp. 2825–2830, 2011.
[30] H. E. Grecco, M. C. Dartiailh, G. Thalhammer-Thurner, T. Bronger, and F. Bauer, “PyVISA: the Python instrumentation package,” *J. Open Source Softw.*, vol. 8, no. 84, p. 5304, Apr. 2023, doi: 10.21105/joss.05304.

Acknowledgements

Part of this work was conducted at the Molecular Analysis Facility, a National Nanotechnology Coordinated Infrastructure (NNCI) site at the University of Washington, which is supported in part by funds from the National Science Foundation (awards NNCI-2025489, NNCI-1542101), the Molecular Engineering & Sciences Institute, and the Clean Energy Institute.

Figure 6 was created with BioRender.com.

Appendix

Appendix A: GitHub Repository for Python Code

The complete code used to process the data, build the models, and interface with the multimeter to collect the data and run the solvent classification and water quantification scripts can be found on this project's GitHub repository. The serialized model and scaler objects can also be found in the repository as *.pkl files. Instructions to run the model and scripts on your own computer are found in the read-me file. https://github.com/gregorymoore2/MastersResearchCode

Appendix B: Video: Live Demonstrations of Solvent Classification

A video demonstration of the strip sensor performing a solvent classification task can be found at the link below.

Solvent Classification with Strip: https://tinyurl.com/yc3eauat

Appendix C: PC620D Hot Plate Characterization

Following the procedure outlined in the methods section, the larger PC620D hot plate was also characterized, and the temperatures reported in the heat map below. This procedure was repeated at two different temperatures, 40°C and 60°C.

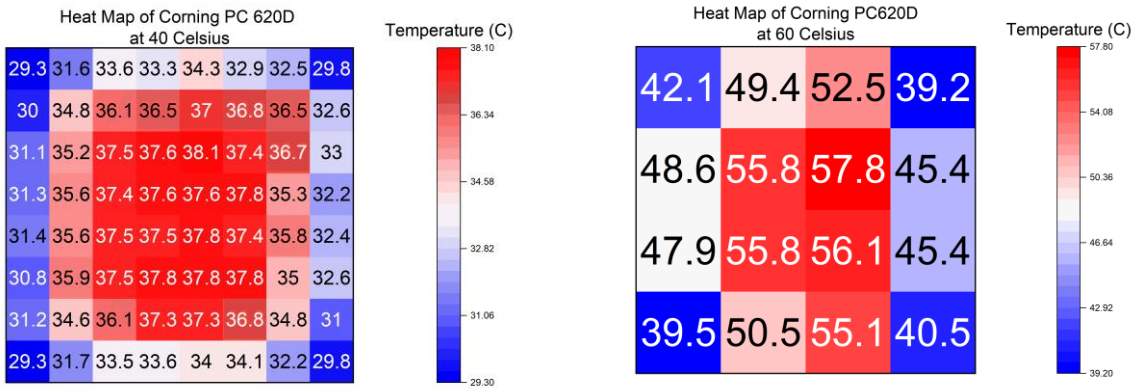

Figure 21. Corning PC620D Hot Plate Heat Map

Appendix D: Data Collection Steps on Keithley

1. Power on the Keithley DMM6500 and plug in a USB drive into the front panel.
2. Connect the sensor under test with alligator clips plugged into the Input HI and Input LO ports on the front panel.
3. Make sure the light on the front panel is on next to “FRONT” this means the data will be collected on the front terminals, if it is set to “REAR”, click in the TERMINALS button.
4. Press the MENU button to the left of the screen.
5. On the touch screen under the “MEASURE” column, press “Quickset” then where it says “Function” change it to 2W resistance.
6. On the same screen on the performance slider click “Activate Control” and slide it over to the left one unit, such that the Resolution reads ~ 6.5 digits and the Speed is ~ 5 rdgs/sec.
7. Click MENU > “Reading Buffers” > debuffer1 > Create New
8. Name the buffer with the name of the set of tests you will be running, i.e. April10th250ppm. Save the name and continue through the settings, Standard and initial capacity 10,000.
9. You are now reading to start a measurement. Click MENU > Graph to bring up the graph.
10. Click the “Scale” tab and under X-Axis Method change it from “Smart Scale” to “Show all Readings”
11. Click the “Data” tab, select the active buffer, and click “Clear Buffer” on the right side of the screen.
12. Now that the buffer has been cleared, wait ~10-15 seconds for the readings to stabilize and then begin your test.
13. When you are finished collecting data, press “MENU” > “Reading Buffers” and “Save to USB”.